



THE INFLUENCE OF TITANIUM DIOXIDE IN THE PVK MATRIX ON ANTI-BACTERIAL PROPERTIES, ELECTRICAL RESISTANCE AND RESISTANCE TO UV RADIATION

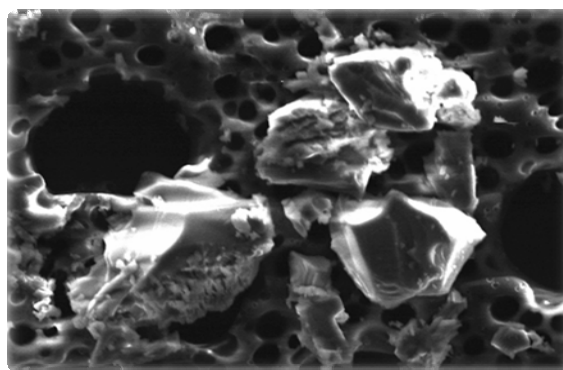
Ouahiba BOURICHE,^{a, b*} Brahim BOUZERAFA,^a Hicham KOUADRI^{a, b*} and Ouarda DJAOUT^b

^a Laboratory: Preparation and Modification of Multiphase Polymeric Materials (LMPMP), Department of Process Engineering, University of Ferhat Abbas Setif 1 19000 Algeria

^b The Center of Scientific and Technical Research in Physicochemical Analyzes (CRAPC), BP384, Industrial Zone Bou_ Ismail RP 42004 Tipaza Algeria

Received June 8, 2017

In the present study the poly (N-vinylcarbazole) (PVK) is doped with nano-crystalline titanium dioxide (TiO₂). The solutions of the PVK-TiO₂ and neat PVK in the DMSO were prepared, followed by a gradual evaporation of the solvent until the mixture became viscous. The viscous solution was drop-cast onto a pre-cleaned glass substrate (ITO). A polymer thin film was formed after slow solvent evaporation under ambient conditions for 12h. Thin films of PVK-TiO₂ composites show a porous microstructure (SEM). The complexation and the ultraviolet resistance of the composite were confirmed by Fourier transform infrared spectroscopy (FTIR) and UV-Visible studies. The antibacterial activity was tested with various concentrations, 10⁻²M, 3.10⁻²M and 5.10⁻²M of doping, with *Bacillus subtilis*, *Pseudomonas aeruginosa*, *Escherichia coli*, and *Staphylococcus*. The electrical resistance of the samples of PVK and these complexes is based on the Automatic Mapping Four Point Probe System. Moreover, the TiO₂ based Poly (N-vinylcarbazole) (PVK) exhibited a remarkable variation at higher concentrations as compared to that of the pure poly (N-vinylcarbazole) film. The antimicrobial activity against gram negative and gram positive bacteria increased with the increase in the concentrations of TiO₂ and the maximum inhibition of bacteria growth was observed in PVK-TiO₂(5.10⁻²M) composites with *Escherichia coli*. This is due to the higher concentrations of TiO₂, activated surface area and better dispersion of TiO₂ on PVK. The results of SEM confirm the presence of TiO₂ in the composite, which consequently modifies the morphology of the film significantly.



INTRODUCTION

Poly (N-vinylcarbazole) (PVK) is a nonconjugated polymer,^{1, 2} and it is a vinyl polymer with repeat carbazole poly cycle. The PVK is an amorphous, thermoplastic, hard and transparent polymer.³

This material has outstanding physicochemical properties (photoconductive, photo-refractive, high

photovoltaic cells, holograms, and photocopies. PVK is a good insulator in the neutral state with low conductivity of about 10⁻¹⁴ to 10⁻¹⁶ S.cm⁻¹, and it was used originally as a dielectric capacitor, since it has very good electrical resistance over a range of temperatures and frequencies.^{4, 5} The PVK has an energy gap (Eg) in the range of 3.3-3.5 eV.^{6, 7} The photoconductive character of PVK (increase in electrical conduction under the influence of light

*Corresponding authors: Tel: (+213) 549 9936 82; E-mail: anesk2011@yahoo.fr; (Dr. BOURICHE Ouahiba); E-mail: chinpolyhim@yahoo.fr; (Dr. KOUADRI Hicham)

exploitation of PVK in the field of xerography and radiation. In addition to its photoconductive power, the PVK is also photo- and electroluminescent.⁹

A number of studies have been carried out on the photodegradation of poly (N-vinylcarbazole) under UV irradiation. Bussi re PO *et al.*¹⁰ studied the photodegradation of poly (N-vinylcarbazole), and Aur lien,¹¹ studied the photochemical behavior upon exposure to UV- light of a poly (2, 7-carbazole) derivative for use in high-performance solar cells. Akira, I, Rivaton. A *et al.* have also followed the evolution of the IR spectrum of a PVK film photooxidized.¹²⁻¹⁴

The organic-inorganic hybrid materials are the subject of much research because they help develop new applications by combining the properties of both components. For two decades, the titanium dioxide films have been extensively studied for many applications including photo catalysis, solar cells, and coatings for optics or wave guide applications of titanium dioxide for the manufacture of integrated optical devices.

Inorganic particles not only increase the mechanical strength of the polymers but also can provide antibacterial property.¹⁵ TiO₂ is one of these agents. It is a semiconductor photo catalyst that can generate hydroxyl radicals (OH) under UV light. This is very important in catalysis reaction, and antibacterial property of TiO₂ comes from the light reactivity of the excited hydroxyl radicals.¹⁶

The work of Robinson *et al.*¹⁷ showed the antibacterial activity of titanium dioxide powder type anatase with *Escherichia Coli* under and in the absence of UV light. This postulate was confirmed by Rincon *et al.*¹⁸ Kubacka *et al.*¹⁹ studied the activity of TiO₂ in an EVOH matrix at different rates (from 0.5 to 5% by mass).

Bahloul W²⁰ studied the antibacterial properties by incorporating titanium dioxide-type (anatase) in a polypropylene matrix. Cheng *et al.*²¹ prepared a composite material from mixing TiO₂-Ag and PVC granules. Su *et al.*²² prepared a nanocomposite TiO₂/Ag/polyethylene glycol (PEG600). The antibacterial activity of a composite film TiO₂/Ag was studied by Liu *et al.*²³ Paulina Rokicka *et al.*²⁴ examined the antibacterial properties of 15 Titania photo catalysts, mono- and dual-modified with nitrogen and carbon. The antimicrobial activity of single-walled carbon nanotubes coated with poly (N-vinylcarbazole) was studied by Ahmed F.²⁵

The aim of our study is to incorporate titanium dioxide (TiO₂) into PVK and to study the TiO₂ concentrations effect on optical absorption, antibacterial

activities, ultraviolet resistance, electrical resistance and morphology of Poly (N-vinylcarbazole). We note that the antibacterial activities and ultraviolet resistance of PVK-TiO₂ have not been studied yet. Therefore, we report the detailed studies here.

EXPERIMENTAL

1. Materials

The following materials were used in this investigation:

Commercially Poly (N-vinylcarbazole) (molecular weight 1,100,000).

Titanium dioxide (TiO₂) powder. The materials were purchased from Sigma-Aldrich and were used without any additional purification.

Dimethylsulfoxide (DMSO) as a solvent.

Gentamicin (10 µg/disc).

Indium Tin Oxide (ITO) coated substrates.

Filter paper discs (5 mm in diameter).

The solid media plates.

Muller Hilton agar was used for bacteria culture; Strains of bacteria were obtained from the American Type Culture Collection.

Four bacterial strains were tested: *Escherichia coli* ATCC 25922, *Pseudomonas aeruginosa* ATCC27853, *Bacillus subtilis* ATCC 6633 and *Staphylococcus aureus* ATCC 43300.

2. Sample Preparation

PVK and TiO₂ materials were dissolved in DMSO at ambient air. The composite was used in a bath deposition onto glass substrates (ITO). To the deposition process, the ITO substrates were ultrasonically cleaned in methanol, acetone and distillate water for 10 min, and the samples were further dried in ambient air for 12h. The thickness of the polymer layer was controlled with the help of different deposition time and by the concentrations of polymer in the solvent (thickness of the order of 5 µm). Muller Hilton agar was used for bacteria culture. Strains of bacteria were obtained from the American Type Culture Collection. Four bacterial strains were tested. Briefly, a suspension of the tested microorganism (0.1 mL 10⁸ cells per mL) was spread on the solid media plates. Filter paper discs (5 mm in diameter) were impregnated with 10 µL of 100 mg/mL of the composite and placed on the inoculated plates. These plates were incubated at 37 C° for 24h. Gentamicin (10 µg/disc) was used as a standard and dimethylsulfoxide DMSO as a control.

CHARACTERIZATION

1. FTIR spectroscopy

In the present study, the chemical structure and the complexation of the composites were investigated by FTIR spectroscopy using an EO-SXB IR spectrometer with a resolution of 4 cm^{-1} in the range $400\text{--}4000\text{ cm}^{-1}$.

2. UV-Visible

The absorption spectra of the films were recorded using a Shimadzu UV-Visible spectrometer.

3. Antibacterial test

In our study, Agar disc diffusion testing,²⁶ was employed for the determination of antibacterial activities of pure PVK and PVK-TiO₂ composite. It is a simple and practical method, and is well-standardized. The test is performed by applying a bacterial inoculum of approximately $1\text{--}2 \times 10^8\text{ CFU/mL}$ to the surface of a 150 mm diameter Mueller-Hinton agar plate. Fixed concentration and paper disks are placed on the inoculated agar surface. Plates are incubated for 16–24 h at 37°C prior to the determination of results. The zones of growth inhibition around each of the disks are measured to the nearest millimeter. The diameter of the zone is related to the diffusion rate of the antibacterial agent through the agar medium.

4. The electrical conductivity

For this, we used a resistivity type CMT-SR 2000N, which is a fully automatic system for measuring the electrical resistance of the conductive layers and semiconductors. The measurement is based on the four-point method. This technique is generally used because of its simplicity and its effectiveness.

5. Ultraviolet Resistance of TiO₂ in the poly(N-vinylcarbazole)materials

In order to prove the ultraviolet resistance of TiO₂ in the Poly (N-vinylcarbazole) materials, the films of PVK, PVK-TiO₂ were exposed to UV light lamp of 32W of which the wavelength was between 300 and 400 nm for 120h and 300h, and the distance between the UV light and the samples was kept at

20 cm. The ultraviolet resistance of TiO₂ in the PVK materials was investigated using an EO-SXB IR spectrometer.

6. Morphological Characterization (Scanning electron microscopy):

Scanning electron microscopy (SEM) is currently the most used in topography on the microscopic scale. A JEOL 7001 F electron microscope (SEM) was used to observe the morphology of PVK, PVK-TiO₂ composites at an accelerating voltage of 12 kV.

RESULTS AND DISCUSSION

UV-Visible Analysis

UV-Visible spectra of pure PVK film and doped TiO₂ Polymer exhibit absorption in ultraviolet region with maximum absorption as shown in Fig. 1. It is clear that the absorbance increases with the increase of TiO₂ concentration in the matrix, and the PVK-TiO₂ composites doped with 5.10^{-2}M of TiO₂ gave higher absorbance value. Results are derived from the charge transfer mechanism between PVK and TiO₂ according to the proper concentration of the pn-heterojunction.^{6,27}

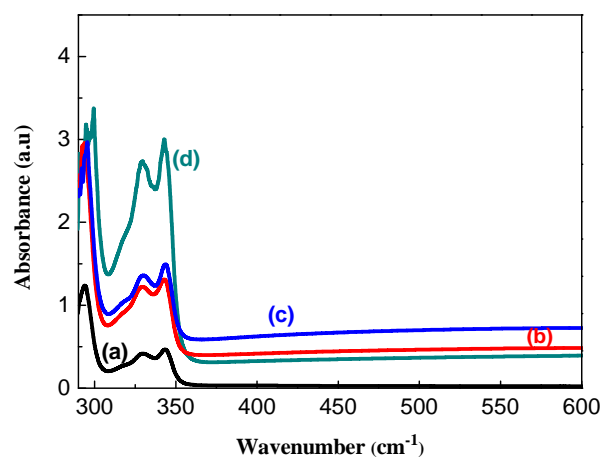


Fig. 1 – UV-Visible spectra of (a) Pure PVK, (b) PVK/ 10^{-2}M TiO₂, (c) PVK/ 3.10^{-2}M TiO₂ and (d) PVK/ 5.10^{-2}M TiO₂.

FTIR analysis

FTIR spectroscopy is a useful tool for determining the extent of the interaction between the polymer and the nanocrystals. Fig. 2 presents the FTIR spectra of PVK, and PVK-TiO₂ showed the following characteristic peaks: The absorption band at 1597 cm^{-1}

is due to the Aromatic C=C stretching frequency of PVK. Peak 1442 cm^{-1} is associated with the vibration deformation of the CH bonds of the aromatic group. The band at 1326 cm^{-1} for pure PVK is attributed to CH_2 deformation.

The band at 1223 cm^{-1} is a sign for C-N stretching of N-vinylcarbazole vibration. The band at 741 cm^{-1} is related to the rocking vibration of CH_2 group. The ring deformation of substituted aromatic structure is observed at 704 cm^{-1} .^{6, 32} However, for the composites PVK- TiO_2 , similar peaks with little variation on the stretching frequencies were observed when compared to the control containing PVK only; However, a slight shift in the C-H stretching frequency, from 3058 cm^{-1} for the pure PVK to 3071 cm^{-1} for the nanocomposite, as well as a decrease in the peak intensity is observed. This therefore suggests that the integrity of the polymer is maintained; nevertheless, some interaction between the polymer and the TiO_2 is still evident and this bodes well with the morphology observed in the SEM. This result is in agreement with the work of Govindraju. S *et al.*²⁸

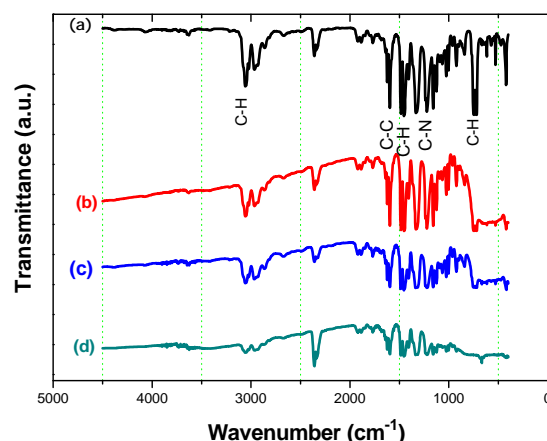


Fig. 2 – IR spectra of : (a) Pure PVK, (b) PVK/ 10^{-2}M TiO_2 , (c) PVK/ 3.10^{-2}M TiO_2 and (d) PVK/ 5.10^{-2}M TiO_2 .

Antibacterial Analysis

The antibacterial activity was determined by measuring inhibition zone diameters (mm) (Fig. 3, and Fig. 4), which were evaluated according to the parameters suggested by Alves *et al.*^{29, 30} (<9 mm: inactive; 9–12 mm: less active; 13–18 mm: active ;> 18 mm: very active).

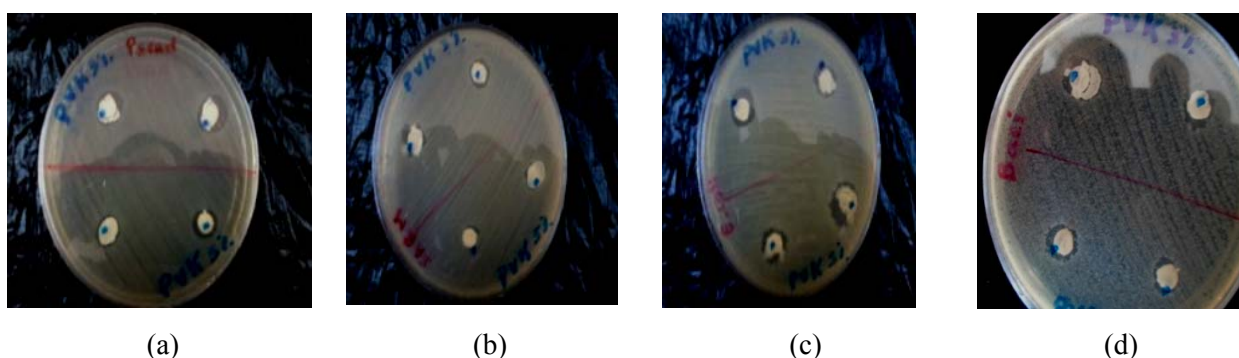


Fig. 3 – Zone of inhibition by different concentrations of PVK/ TiO_2 against (a): *Pseudomonas aeruginosa*, (b): SARM, (c): *Escherichia coli*, (d): *Bacillus subtilis*.

The inhibition zones of the antibacterial activity of PVK pure and doped with 10^{-2}M TiO_2 , 3.10^{-2}M TiO_2 , 5.10^{-2}M TiO_2 and the control test are reported in Table 1.

Table 1

Inhibition zones in millimeter of the antibacterial activity of Poly (N-vinylcarbazole) pure and doped with 10^{-2}M , 3.10^{-2}M , 5.10^{-2}M TiO_2 and control

	<i>Escherichia coli</i> ATCC 25922	<i>Bacillus subtilis</i> ATCC 6633	<i>Pseudomonas aeruginosa</i> ATCC27853	<i>Staphylococcus aureus</i> ATCC43300
Control test	No inhibition	No inhibition	No inhibition	No inhibition
Poly(N-vinylcarbazole) pure	No inhibition	No inhibition	No inhibition	No inhibition
Poly(N-vinylcarbazole) + 10^{-2}M TiO_2	6.50 ± 0.41	6.33 ± 0.41	6.23 ± 0.41	5.88 ± 0.41
Poly(N-vinylcarbazole) + 3.10^{-2}M TiO_2	7.33 ± 0.24	8.01 ± 0.24	7.04 ± 0.24	6.00 ± 0.24
Poly(N-vinylcarbazole) + 5.10^{-2}M TiO_2	9.58 ± 0.24	7.58 ± 0.24	8.11 ± 0.24	6.71 ± 0.24

Results were expressed as the mean \pm standard deviation.

The antimicrobial activity against gram negative and gram positive bacteria increased with the increase in the concentration of TiO_2 , and the maximum inhibition of bacteria growth was observed in PVK- TiO_2 5.10^{-2}M composites. This is due to the higher concentration of TiO_2 , to the activated surface area and the better dispersion of TiO_2 in PVK (confirmed with SEM). The zone of inhibition was not observed in pure PVK, which indicated that the essential activity is due to the TiO_2 concentration.³³

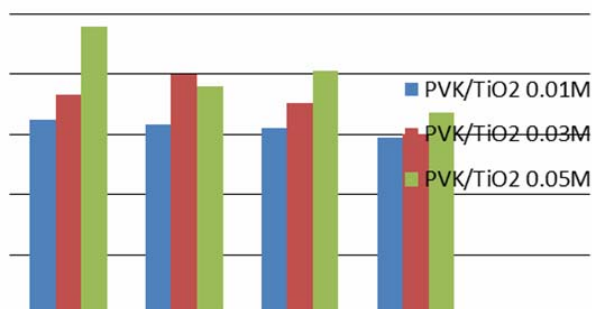


Fig. 4 – Antibacterial activity against gram positive and gram negative bacteria of PVK+ 10^{-2}M TiO_2 , PVK+ 3.10^{-2}M TiO_2 , PVK+ 5.10^{-2}M TiO_2 .

Ultraviolet resistance of TiO_2 in the Poly (N-vinylcarbazole) materials

a) Influence of the irradiation time on PVK

The effects of (UV) light irradiation on pure PVK compared with control device (PVK) without UV light irradiation have been investigated. Fig. 5 and Fig. 6 show IR spectra of pure PVK polymer thin films without and with UV irradiation at 300 and 400 nm for 120h and 300h at 25°C.

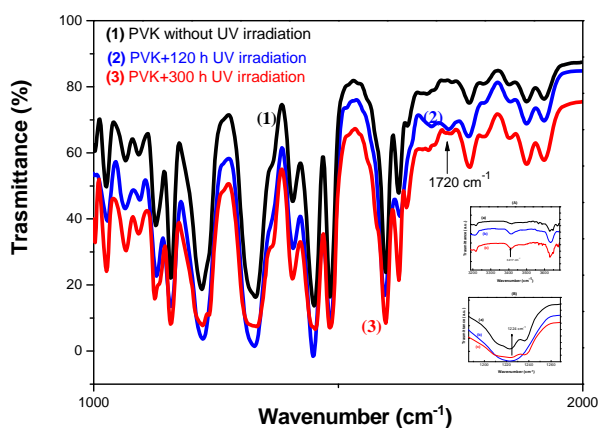


Fig. 5 – Comparison of IR spectra of pure PVK polymer thin films (5 μm) caused by photolysis irradiation time at (300 and 400 nm) for 120h and 300h at 25°C°.

Intensities of the binding energy peaks increased as the time of UV irradiation increased (120h and 300h). These suggest that the scission of molecular chain of PVK developed, such result had been already reported by Rivaton *et al.*¹⁴ and the density of states in valence band increased as the time of UV irradiation increased. An irradiated PVK film should also be photolysed long (over 100 hours of irradiation) prior to observing significant developments in infrared spectrum. Firstly, the changes are mainly observed with appearance of two peaks one at 1720 cm^{-1} corresponding to carbonyl groups and the other at 3417 cm^{-1} , which was attributed to the vibration of the N-H bond of a primary amine (symmetrical elongation). At the same time we observe a decrease in intensity of all bonds characteristic of aromatic cycle ($1450, 1480, 1595, 1623, 1850, 1880, 1920, 3080, 3058, 3022\text{ cm}^{-1}$), a decrease in the intensity of the band at 1224 cm^{-1} corresponding to the breaking of the C-N bond and a lower aliphatic CH.¹⁰⁻¹⁴

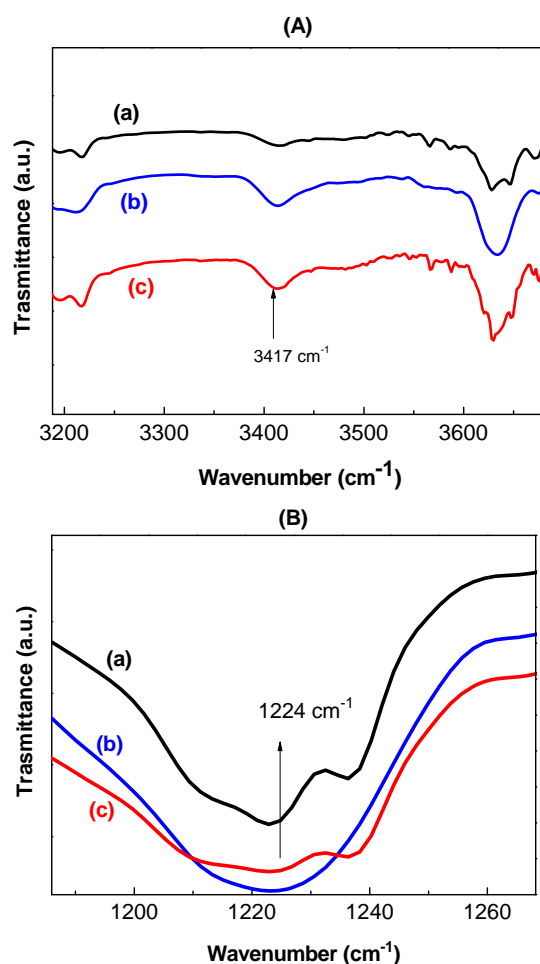


Fig. 6 – Changes in the IR spectra of (a) PVK film (5 μm), (b) PVK film (5 μm) caused by photolysis for 120h at 25°C, (c) PVK film (5 μm) caused by photolysis for 300h at 25°C for: (A) Evolution of the IR spectra in the $3200\text{-}3700\text{ cm}^{-1}$ region, (B) Evolution of the IR spectra in the $1200\text{-}1260\text{ cm}^{-1}$ region.

b) Influence of addition of TiO₂ on photodegradation of PVK

Fig. 7 and Fig. 8 illustrate infrared spectra of pure PVK and PVK-TiO₂ before and after exposure to UV irradiation for 120h and 300h at 25°C (1500-2000cm⁻¹ region) and (2000-3600cm⁻¹ region).

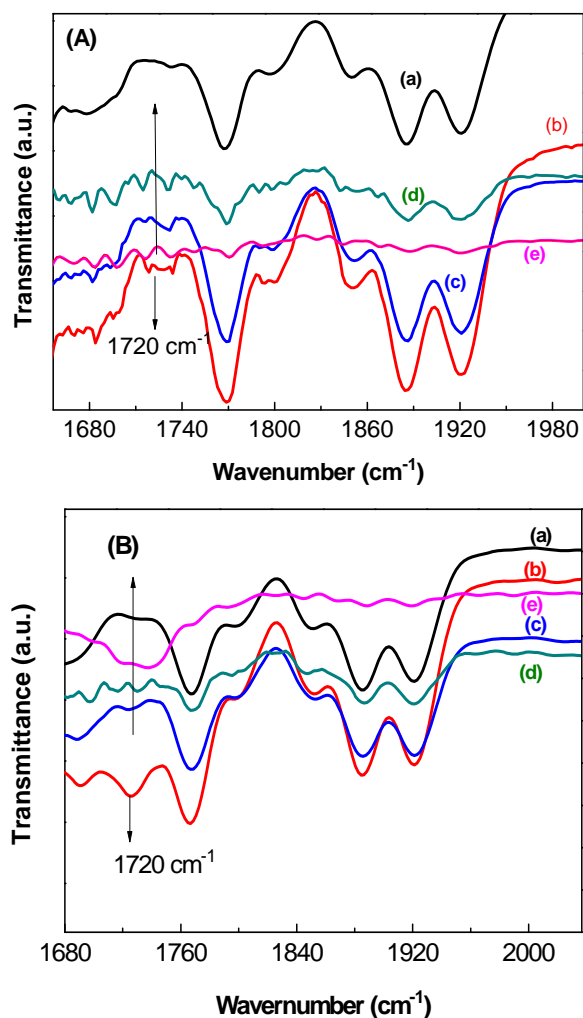


Fig. 7 – Evolution of the IR spectra in the 1500-2000cm⁻¹ region of : (a)- pure PVK film ,(b)-PVK+UV irradiation,(c)- PVK+UV irradiation+10⁻²M TiO₂,(d)- PVK+UV irradiation+3.10⁻²M TiO₂,(e)- PVK+UV irradiation+5.10⁻²M TiO₂ at 25°C photolysis (A) :120h at 300-400 nm, (B) : 300h at 300-400 nm.

The evolution of the absorption bands at 1720 and at 3417cm⁻¹ from FTIR analysis showed that UV-irradiation induced significant photodegradation for PVK. However, with the incorporation of TiO₂ nanoparticles into the PVK materials, the extent of the photodegradation was significantly reduced due to the UV light screening effects offered by the TiO₂ nanoparticles (Fig. 7, 8) and by the concentration of TiO₂. We can note that the TiO₂

nanoparticles absorb the UV radiation and hence reduce the UV intensity, thus promoting the significant improvements on the photodegradation resistance of PVK-TiO₂ to UV-irradiation.

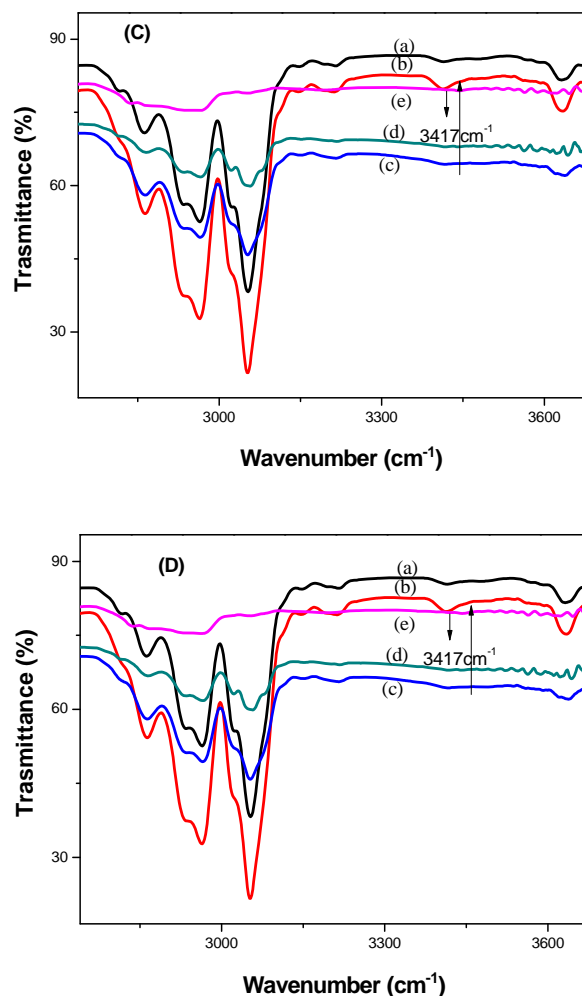


Fig. 8 – Evolution of the IR spectra in the 2000-3600cm⁻¹ region of : (a)- pure PVK film ,(b)-PVK+UV irradiation,(c)-PVK+UV irradiation+10⁻²M TiO₂, (d)-PVK+UV irradiation+3.10⁻²M TiO₂, (e)- PVK+UV irradiation+5.10⁻²M TiO₂ at 25°C photolysis (C) :120h at 300–400 nm, (D) : 300h at 300–400 nm.

Electrical resistance measurement (DC electrical conductivity)

The electrical resistance (ER) and electrical conductivity of PVK, PVK-TiO₂ composite before and after being exposed to UV irradiation obtained by the four-point method are reported in (Table 2 and Fig. 9).

Electrical resistance measurement (DC electrical conductivity)

The electrical resistance (ER) and electrical conductivity of PVK, PVK-TiO₂ composite before and after being exposed to UV irradiation obtained by the four-point method are reported in (Table 2 and Fig. 9).

Table 2

Electrical resistance (ER) and electrical conductivity of PVK, PVK-TiO₂ without and with UV irradiation at 300 and 400 nm for 120h and 300h at 25°C

Sample	Electrical resistance (ER) ($\Omega \cdot \text{cm}$)	(DC electrical conductivity)(S/cm)
PVK pure	2.42E+04	4.13-05
PVK 10 ⁻² M TiO ₂	1.13E+04	8.85-05
PVK 3.10 ⁻² M TiO ₂	1.23E+04	8.13-05
PVK 5.10 ⁻² M TiO ₂	1.51E+04	6.62-05
PVK pure at 120h (UV- R)	2.36E+04	4.23-05
PVK 10 ⁻² M TiO ₂ at 120h(UV- R)	1.51E+04	6.62-05
PVK 3.10 ⁻² M TiO ₂ at 120h(UV- R)	1.35E+04	7.40-05
PVK 5.10 ⁻² M TiO ₂ at 120h (UV- R)	1.54E+03	6.49-04
PVK pure at 300h (UV- R)	2.34E+04	4.27-05
PVK 10 ⁻² M TiO ₂ at 300h(UV- R)	1.81E+04	5.52-05
PVK 3.10 ⁻² M TiO ₂ at 300h(UV- R)	9.20E+03	1.08-04
PVK 5.10 ⁻² M TiO ₂ at 300h(UV- R)	1.44E+03	6.94-04

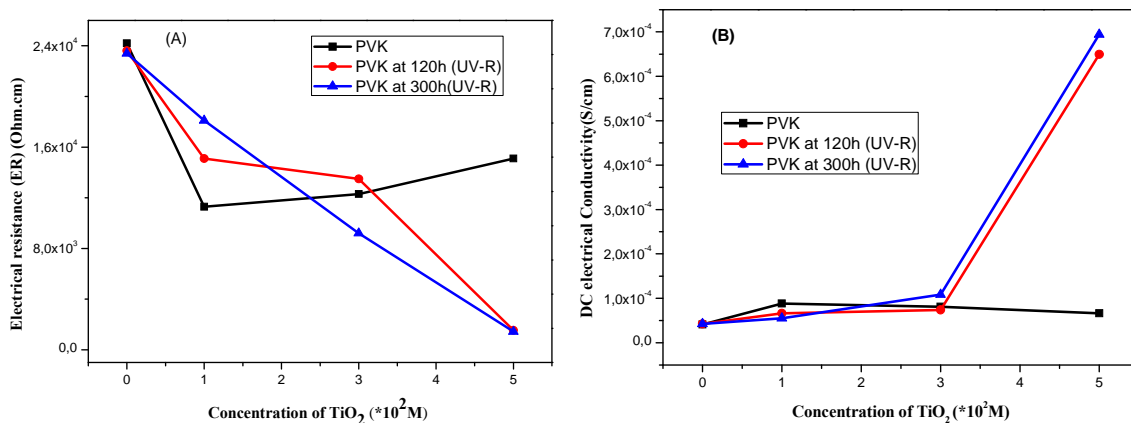


Fig. 9 – (A) Electrical resistance (ER), (B) DC electrical conductivity (S/cm) of PVK, PVK/TiO₂ without and with UV irradiation at 300 and 400 nm for 120h and 300 h at 25°C.

The values of the resistances are comparable to those found in the literature.^{5,31} Moreover, the electrical resistance (ER) decreased with the increasing of the concentration of TiO₂. This decrease is significant at 300 hours of exposure of the PVK to UV irradiation.

The exhibition of PVK to UV irradiation also makes it conductive. The PVK is the first known polymeric photoconductor. The absorption of radiation

generates charge carriers whose displacement is responsible for the conductivity. Poly (N-vinyl-carbazole) is a transporter of holes. These “holes” are related to the cationic radicals delocalized on the carbazyls. The displacement is done by electron jump between nuclei carbazyls of the same chain or of similar chains. PVK is a photo-conductor intrinsic in the ultraviolet wavelength range. It is possible to obtain a photo-

conductor in the visible from PVK by addition of a pigment or electron accepting molecule.

Morphology of thin films properties as function of TiO₂ concentration

Fig. 10 shows SEM images of TiO₂ samples, and a monodispersion of nanoparticles with an average particle size of about 15 to 20 nm can be seen. Consequently, the TiO₂ nanoparticles have a spherical shape.

Fig. 11 (a) represents the microstructure of the PVK thin films with pores and with high

connectivity which are clearly observed. Macropores can be evaluated as almost cylindrical cavities with an average diameter of 500 nm. Fig. 11 (b) and 11 (c) shows the SEM images of PVK-TiO₂ samples. As shown by the micrographs, the TiO₂ nanoparticles are strictly confined in the pores and the occupancy rate depends largely on the concentration. When the concentration of TiO₂ largely dominates ($5 \cdot 10^{-2} M$), the clusters of supersaturated nanoparticles grow on top of the pores where further maturation occurs by diffusion into and from the polymer network, as can be seen from Figure 11(d).³⁴

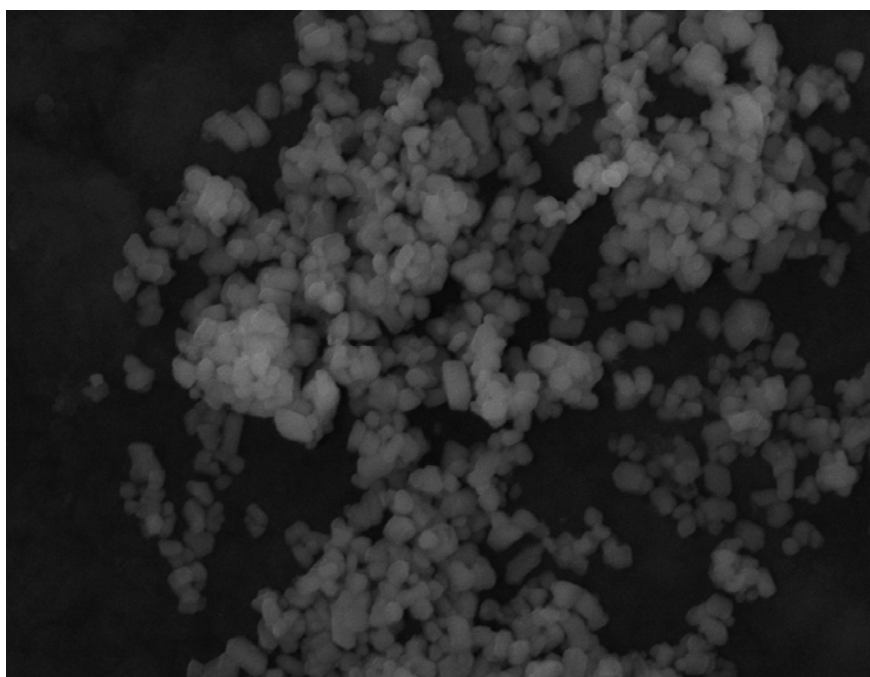
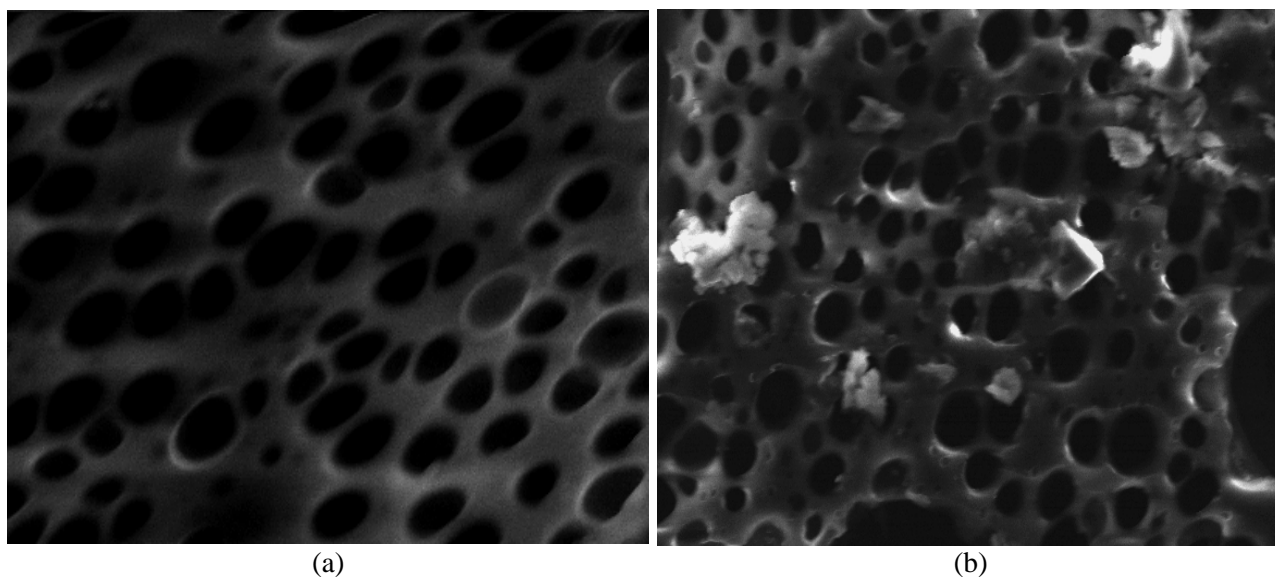


Fig. 10 – SEM image of TiO₂ nanoparticles.



(a)

(b)

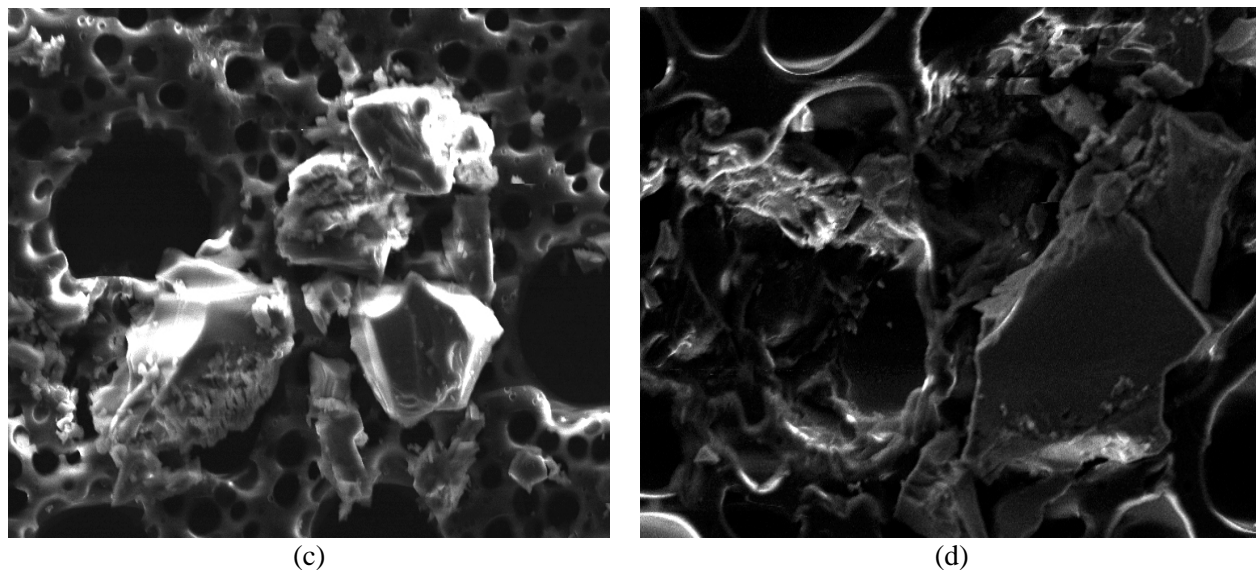


Fig. 11 – SEM image of: (a) pure PVK; (b) PVK: 10^{-2} M TiO₂; (c) PVK: $3 \cdot 10^{-2}$ M TiO₂; and (d) PVK: $5 \cdot 10^{-2}$ M TiO₂ thin films.

CONCLUSION

The aim of the present work was to study the influence of the concentration of TiO₂ inside a PVK matrix via a bath deposition method onto the glass substrates (ITO). For this purpose, the FTIR and UV-visible techniques were used to confirm the complexation of the composite.

The Electrical resistance values are on average comparable to those found in the literature. The sample PVK-TiO₂ $5 \cdot 10^{-2}$ M exhibits higher antibacterial activity against *Escherichia coli*. The chemical structure of TiO₂ and the fine morphology and a good dispersion of the particles in the matrix could explain the bactericidal activity of the PVK-TiO₂ composite.

Photodegradation of a film PVK causes significant change in its infrared spectrum after exposure to UV. This leads to an increase in conductivity and a decrease in resistivity. We can note that the addition of TiO₂ particles absorbs the UV irradiation and hence reduces its effect on the material, thus promoting the significant improvements on the photodegradation resistance of PVK-TiO₂ to UV-irradiation.

REFERENCES

1. J. L. Martin, J. D. Bergeson, V. N. Prigodin and A. J. Epstein, *Synthetic. Met.*, **2010**, *160*, 291-296. A. Kumasi, YI. H and A. Iraqi, *J. Polym. Sci. A1.*, **2007**, *45*, 5957-5967.
2. J. V. Grazulevicius, P. Stroehriegl, J. Pielichowski and K. I. Pielichowski, *Prog. Polym. Sci.*, **2003**, *28*, 1297-1353.
3. S.Oh. Kyoung, B. Won and K. Hwayong, *Polymer.*, **2007**, *48*, 1450-1454.
4. N. Ballav and M. Biswas, *Synthetic Met.*, **2003**, *132*, 213-218.
5. H. Yangang, Wu. Gang, Ch. Hongzeng and W. Mang, *J. Appl. Polym. Sci.*, **2008**, *109*, 882-888.
6. E. Pérez-Gutiérrez, M. J. Percino, V.M. Chapela and J. L. Maldonado, *E. Thin Solid Films*, **2011**, *519*, 6015-6020.
7. S. Touihri, J. C. Bernède, P. Molinie and D. Legoff, *Polymer.*, **2002**, *43*, 3123-3129.
8. Tu. Ming-Lung, Su. Yan-Kuin, Wu. Shang-Shang, Gu.Tzung-Fang, W. Ten-Chin and H. Chun-Yuan, *Synthetic. Met.*, **2011**, *161*, 450-454.
9. B. Pierre-Olivier, R. Agnes, T. Sandrine and G. Jean-Luc, *J. Phys.Chem B.*, **2012**, *19*, 116(2), 802-812.
10. T. Aurélien, B. Pierre-Olivier, W.W.Ch. Pascal, T. Sandrine, R. Agnès, G. Jean-Luc, B. Serge and L. Mario, *Adv. Energy Mater.*, **2013**, *3*, 478-487.
11. I. Akira, O. Ken-Ichi and K. Shig Kazu, *B. Chem. Soc. Jpn.*, **1979**, *52*, 2218.
12. R. F. Cozzens, *J. Am. Chem. Soc.*, **1981**, 137.
13. A. Rivaton, B. Mailhot, G. Derderian, P. O. Bussiere and J. L. Gardette, *Macromolecules*, **2003**, *36*, *15*, 5815-5824.
14. W.Zhaobo, Li. Guicun, P. Hongrui and Z. Zhikun, *Mater. Sci.*, **2005**, *40*, 6433.
15. V. Prashant and Kamat, *Chem. Rev.*, **1993**, *93*, 267-300.
16. M. C. R. Jeanette, K. J. R. Peter and A. L. Linda, *A: Chemistry*, **2005**, *175*, 51-56.
17. A. G Rincon and C. Pulgarin, *Appl. Catal. B-Environ.*, **2003**, *44*, 263-284.
18. A. Kubacka, M. Ferrer, A. Martinez-Arias and M. Fernandez-Garcı, *J. Amer. Chem. Soc.*, **2007**, *7*, 2529-2534.
19. W. Bahloul, M. Flavien, B. L. Véronique and C. Philippe, *Mater. Chem. Phys.*, **2012**, *134*, 399-406.
20. Q. Cheng, C. Pavlinek, S. Li, P. Vladmir, S. Petr and W. Huanbing, *Appl. Surface. Sci.*, **2010**, *252*, 4154-4160.
21. W. Su, S. S. Wei, S. Q. Hu. J. X Tang and J. Hazard, *Mater.*, **2009**, *172*, 716-720.
22. Y. Liu, X. Wang, F. Yang and X. Yang, *Micropor. Mesopor. Mat.*, **2008**, *114*, 431-439.

23. R.O. Paulina, M. S. Agata, K. Lukasz, K. Ewa and W. M. Antoni., *Pol J Chem Technol.*, **2016**, *18*, 56–64.
24. F. Ahmed, C. M. Santos, R. A. M. V. Vergara, M. C. R. Tria, R. Advincula and D. F. Rodrigues, *Environ. Sci. Technol.*, **2012**, *46*, 1804-1810.
25. A. Alves, T. M. Silva, A. F. Brandão, M. Grandi, T. S. M. Smânia, E. F. A. Smânia and Jr. A. Zani, *Mem. I. Oswaldo. Cruz.*, **2000**, *95*, 367–373.
26. W. L. Sang and H.C. Seung, *Sensors.*, **2016**, *16*, 1, 74.
27. S. Govindraj, N. Ntholeng, K. Ranganathan, M. J. Moloto, L. M. Sikhwivhilu and N. Moloto, *J. Nanomater.*, **2016**, 9592189, 8.
28. S. Gaamoune, W. Nouioua and O. Djaout, *A. J. B. P. A. D.*, **2015**, *3*, 2231-2560.
29. S. Ankita, D. Amit and K. Rajnish, *J. Porous. Mater.*, **2016**, *23*, 851–855.
30. C. Basavaraja, Jo. EunAe, K. Bong Sung, H. Mallikarjuna and H. Do. Sung, *Bull. Korean.Chem. Soc.*, **2010**, *31*, *10*, 2967.
31. M. Catherine, K. M Santos and A. CuiFarid, *Macromol. Mater. Eng.*, **2012**, 77204-5003.
32. A. Razi and S. Meryam, *I.J. I. R. S. E. T.*, **2013**, *2*, *8*, 2319-8753.
33. A. Benchaabane, Z. Ben Hamed, F. Kouki, M. A. Sanhoury, K. Zellama, Z. Andreas and H. Bouchriha, *J. Appl. Phys.*, **2014**, *115*, 134313.